Hyperbranched polyglycerol coated vascular stents – a non-pharmacological approach to reducing device-triggered thrombosis and restenosis

Eli Moore (✉ Eli.moore@unisa.edu.au)

SA Pathology   https://orcid.org/0000-0002-4131-8299

Michaelia Cockshell

SA Pathology

Victoria Nankivell

South Australian Health and Medical Research Institute

Anouck Burzava

University of South Australia

Markus Tondl

University of South Australia

Glen Benveniste

Ashford Vascular

John Finnie

University of Adelaide

Peter Psaltis

South Australian Health and Medical Research Institute

Hans Greisser

Future Industries Institute, University of South Australia

Christina Bursill

University of Adelaide

Nicolas Voelcker

Monash University   https://orcid.org/0000-0002-1536-7804

Tony Simula

TekCyte

Claudine Bonder

University of South Australia

Article

Keywords:

Hyperbranched polyglycerol coated vascular stents – a non-pharmacological approach to reducing device-triggered thrombosis and restenosis

Eli Moore[1], Michaelia P. Cockshell[1], Victoria Nankivell[2], Anouck L. S. Burzava[3], Markus Tondl[1], Glen Benveniste[4], John W. Finnie[5], Peter J. Psaltis[2,5,6], Hans J. Griesser[3], Christina A. Bursill[2], Nicolas H. Voelcker[7,8,9], Tony Simula[10], Claudine S. Bonder[1,5]

[1]Centre for Cancer Biology, University of South Australia and SA Pathology, Adelaide, South Australia, 5000, Australia

[2]Vascular Research Centre, Heart and Vascular Program, Lifelong Health Theme, South Australian Health and Medical Research Institute, Adelaide, South Australia, 5000, Australia

[3]Future Industries Institute, University of South Australia, Mawson Lakes, South Australia, 5095, Australia

[4]Ashford Vascular, Ashford, South Australia, 5035, Australia

[5]Adelaide Medical School, University of Adelaide, South Australia, 5000, Australia

[6]Department of Cardiology, Central Adelaide Local Health Network, Adelaide, South Australia, 5000, Australia

[7]Monash Institute of Pharmaceutical Sciences, Monash University, Parkville, Victoria, 3052, Australia

[8]Melbourne Centre for Nanofabrication, Victorian Node of the Australian National Fabrication Facility, Clayton, Victoria, 3168, Australia

[9]CSIRO Manufacturing, Clayton, Victoria, 3158, Australia

[10]TekCyte Limited, Mawson Lakes, South Australia, 5095, Australia

Synthetic materials with an innate ability to avoid the foreign-body-response remain an unrealized goal that would transform the medical device industry. The balance of bulk material properties, that enable a device to perform as intended, with surface properties, that provide bio- and hemocompatibility, has always required the former to be prioritized. While all materials used in modern devices have an acceptable level of biocompatibility, imperfection remains, ultimately leading to device failure, or requiring pharmacological intervention for it to be tolerated. Where such devices cause damage or place strain on the normal architecture of the surrounding tissue, these impacts may initiate inflammatory responses that can also led to failure. This is most evident in the treatment of vessels in the lower extremity in patients with peripheral arterial disease (PAD), where in-stent restenosis (ISR) remains a significant challenge for vascular surgeons. Blood-contacting devices, such as stents and artificial grafts, are considered particularly difficult to shield from the foreign-body-response due to the immediate and direct exposure to blood and therefore, the full gamut of the body's immune responses. Pharmacological treatment is currently paramount to successful percutaneous vascular intervention (PVI) with antiplatelet therapies being prescribed to manage the risk of thrombosis and cytotoxic drug-eluting coatings to reduce restenosis. Here, we present data that indicate a nano-thin coating of hyperbranched polyglycerol (HPG) can greatly improve the safety and durability of endovascular metal stents. The HPG coating successfully prevents the binding and activation of platelets and greatly reduces the thrombogenicity of nitinol stents when studied *ex vivo*, using fresh human blood. *In vivo*, HPG-coated stainless-steel stents remained patent after 28 days in apolipoprotein E (ApoE) knockout mice while control stents all became completely occluded, highlighting the HPG coating's ability to reduce restenosis. Together, these properties could help alleviate the industry's dependence on blood-thinning and antiproliferative drugs to resolve device compatibility issues; thereby greatly improve patients' quality of life through faster recovery, fewer complications and fewer repeat interventions. Furthermore, this coating technology is compatible with a range of materials commonly used in the production of implantable medical devices, such as stainless steel, nitinol, silicone, and polytetrafluoroethylene, while being highly scalable, cost effective and stable. Taken together, HPG presents itself as an alternative coating suitable for a broad range of vascular devices including stents and grafts.

The introduction of vascular stents provided surgeons with significant and meaningful tools in the fight against the ever-increasing epidemic that is cardiovascular disease.[1] The ability to physically reopen and maintain patency in diseased and occluded vasculature has saved countless lives. Furthermore, generational refinements have made great strides in improving the efficacy of vascular stents.[2] However, all implanted materials elicit a foreign-body-response to varying degrees that carry associated risks which have never been fully overcome, even with the use of materials that meet current biocompatibility standards.[3] In the case of endovascular stents, exposure to blood results in rapid adhesion of proteins and cells, initiating a cascade of events that can lead to stent thrombosis (ST). This can be a life-threatening complication, often requiring emergency intervention, which can also lead to amputations or death. The physiological processes behind the thrombogenic response to stents are well understood and documented

for decades.[4] However, as yet, a suitable materials engineering solution to evade these complex and highly evolved processes has not been developed.

Current best practice following implantation of vascular stents includes the long-term prescription of antiplatelet, blood-thinning medications to reduce the likelihood of ST. As with many pharmacological approaches, the administration of dual antiplatelet therapy (DAPT) for durations of several months to years, can have serious side effects, including upper gastrointestinal bleeding, ecchymosis, hematuria and epistaxis, resulting in greatly reduced quality of life for patients.[5, 6] The ongoing use of DAPT also makes follow-up and emergency procedures potentially fatal due to the high risk of increased bleeding during surgery. However, patients who cease antiplatelet medications early, to perform scheduled surgery, have an elevated risk of ST and perioperative myocardial infarction.[7, 8]

In-stent restenosis (ISR) is another immune-triggered complication leading to vessel re-occlusion, that develops over months, requiring further intervention and possibly surgery.[9-11] This is particularly evident in peripheral arterial disease where reported rates of ISR have been as high as 40% in some patient populations in the first 12 months after treatment with a stent.[12-14] After vascular injury from insertion of a stent, inflammatory factors are released by several cell types including platelets, macrophages and lymphocytes.[15] These factors lead to the secretion of growth factors that increases the proliferation and migration of vascular smooth muscle cells into the intimal region, leading to intimal hyperplasia and ISR.[16, 17]

Drug-eluting stents (DES) have been the industry's solution to this problem, with cellular proliferation put on hold for as long as the drug continues to leach from the stent. This approach has had varied levels of success, and is considered the gold standard at present, but is limited by the finite therapeutic duration.[18] Exposed stent struts and polymer coatings, that act as reservoirs for the drug, can also trigger late thrombotic events after the therapeutic window has expired.[19] There have also been reports of higher rates of all-cause mortality and amputations in patients with peripheral arterial disease treated with paclitaxel-coated devices, compared with uncoated devices.[20-22]

It is clearly of paramount importance that a new generation of vascular stents contain the intrinsic ability to prevent the foreign-body-response leading to ST and ISR without the need for ongoing and long-term pharmacological intervention. To achieve this, surface properties of the devices must include the ability to prevent undesired protein and platelet attachment as well as provide an environment conducive to the healing of damaged vessel walls and reduce the likelihood of restenosis. Numerous stent coating approaches have been studied which have included a range of organic polymers, inorganic films, and biological components.[23] Each approach managing to demonstrate improvements in some respects. However, despite great advancements in the field, the ideal stent remains elusive.

Hyperbranched polyglycerol (HPG)-grafted substrates have already demonstrated very effective resistance to surface adhesion of a range of proteins and cells by us and others.[24-29] Furthermore, the biocompatibility and hemocompatibility of HPG in solution have been documented, with *in vitro* and *in vivo* assays indicating HPG has no adverse effects on complement activation and platelet activation.[30-33] Despite the promising evidence for clinical application, the biocompatibility, hemocompatibility and durability of HPG on vascular devices, have not been extensively tested. This has been in part due to the considerable limitations with previous methods of achieving a commercially viable HPG coating on materials, which were complex, costly and involved many hazardous chemicals.[26, 34-37] We sought to overcome these limitations with a novel coating process that is simple, environmentally friendly and commercially viable. The promising results obtained with HPG coatings in previous studies along with advances in the coating technology suggested that a comprehensive evaluation was warranted of the extent to which the HPG coating may prevent adverse responses by the various components and systems of the cardiovascular environment. The data we generated suggest our new HPG-grafting technology has made possible the potential to provide a superior biocompatibility and hemocompatibility medical coating to improve patency and durability of peripheral vascular devices.

RESULTS

HPG prevents platelet adhesion and activation

Platelet binding and activation is one of the first defenses in the foreign-body-response.[4] We began testing the hemocompatibility of HPG-grafted materials by investigating the interaction with freshly isolated human platelets, so as to decouple this reaction from other protein and cellular responses to the surfaces. In line with our previous work, HPG was grafted from polystyrene (PS), Figure 1, that had been spin-coated onto a silicon wafer to allow for easy chemical (SI Table 1 and SI Figure 1) and biological analysis of the flat and pure substrate. The HPG coating was characterized by between 60% and 90% etheric carbon (C-O-C) groups on high resolution C1s spectra, which is consistent with the literature.[38] Isolated platelet suspensions from human volunteers were incubated on the surfaces for 1 hour, washed and stained. Platelets were found to bind in abundance to the plasma-treated PS controls, as seen in Figure 2a. This was not unexpected as these surfaces are analogous to tissue culture polystyrene and highly susceptible to cell attachment. Conversely, the HPG-grafted PS was found to be extremely resistant to platelet binding, which was reduced by >99.99%, with respect to the PS control (p<0.0001). Interestingly, multiple morphologies were observed for the bound platelets that ranged from small and rounded through to large and spread with pseudopodia. For analysis, the platelets were categorized into three distinct subpopulations and partitioned by visual assessment from the fluorescent micrographs, as summarized in Figure 2b. These morphologies are a reliable indicator of the state of activation of the platelets, with greater cell spreading associated with greater activation.[39, 40] Small rounded platelets are considered to be in a nonactivated resting

state.[41] The PS controls consisted of ~84% of platelets that were completely spread, ~6% that were starting to spread (dendritic morphology) and ~10% that remained round. It is our contention that a vast majority of the platelets bound to the PS were activated and would be contributing to thrombus formation in a whole-blood system.[42] There were no spread platelets found on the HPG-coated samples. This data suggest that the HPG coating almost completely prevented platelet attachment and activation in this isolated system.

Flat substrates are often necessary to validate the performance of a medical coating but they do not comprise the technically challenging aspects associated with three-dimensional and multifaceted devices, such as stents. Moving towards a more geometrically complex model system, stainless-steel (SS) mesh, with 90 μm thick woven wires, was chosen to represent a more stent like architecture. HPG modification of SS mesh followed the same process as for flat PS (Figure 1) and yielded the characteristic etheric carbon peak expected for a suitable HPG coating (SI Table 1 and SI Figure 1). Following incubation with isolated platelets, washing and staining, the control SS mesh was clearly visualized by fluorescence microscopy due to the abundance of bound platelets, Figure 2c. Once again, it was not unexpected that large quantities of platelets would bind to the uncoated control samples since this is a known limitation of clinical-grade SS stents.[43] On the other hand, the HPG-grafted SS mesh exhibited very few platelets (99.8% reduction over control, calculated by fluorescent area over equivalent fields of view), despite the increased complex geometry and potential places for the platelets to lodge. Notably, the few bound platelets on the HPG-coated SS mesh were not associated with any particular feature of the woven mesh, such as the cross-over joints, as might have been expected. Achieving this very low binding of platelets on a substrate with much greater geometric complexity and on a material of clinical relevance is a testament to the robustness and potential for an HPG coating to provide benefits to existing endovascular devices. The result also confirms the uniformity of our HPG coating process, able to protect the more hidden surfaces at the cross-over joints.

HPG prevents stent thrombosis *ex vivo*

Building on the reduced platelet binding on SS mesh, the HPG coating was further challenged on clinical-grade nitinol stents using whole blood under conditions of shear flow (Figure 3). Here, we investigated ST in HPG-grafted nitinol stents exposed to fresh human blood, using a modified Chandler loop assay.[44, 45] For these studies, commercially available 6 mm diameter stents were cut into sections consisting of 4 struts and coated with HPG following the same process as previous substrates (Figure 1). Successful HPG grafting was confirmed by a characteristic etheric carbon peak in the high resolution XPS spectra (SI Table 1 and SI Figure 1). This process results in the polymer being covalently bound to the stent surface and along with being several nanometers thick, this alleviates issues with delamination encountered by dip and spray coating techniques.[46]

A typical Chandler loop assay consisted of one bare (control) stent section and up to four HPG-grafted stent sections inserted into separate loops, which were then filled with fresh blood. Simulated blood flow was maintained in each loop at approximately 5 dyn/cm^2 at 37°C for 2 hours. A representation of the outcome of these assays is presented in Figure 3b and shows a significant difference in performance between bare nitinol and HPG-grafted nitinol stent sections. Every bare nitinol control was completely occluded by the completion of the assay, however, clots varied in size and weight between donors. In stark contrast, the HPG-grafted stent sections consistently appeared free from any clot formation and weighed significantly less than the controls (Figure 3c). To interrogate further and identify any cellular interactions that might be occurring at the surface, scanning electron microscopy (SEM) images of the stent samples were analyzed. As expected, in Figure 3d, the control stents were completely covered in large networks of fibrin strands containing trapped erythrocytes, which were absent from HPG-grafted stent sections (Figure 3d). This was consistent with the reduced platelet binding on HPG-coated surfaces and supports the hypothesis that the prevention of platelet binding reduces thrombosis on HPG-grafted stents. The SEM micrographs did however uncover the presence of a population of cells lining, almost exclusively, the area of the stent struts that lay perpendicular to the direction of blood flow (Figure 3e). These areas are known to create eddies in the flowing blood and potentially cause the blood to stagnate at these locations.[47] Whilst platelets and erythrocytes could be ruled out due to the size and shape of the cells, the nature of these cells could not be determined from the SEM micrographs. However, fluorescence microscopy revealed the population consisted of lobulated mononuclear cells (Figure 3f), consistent with neutrophils. Furthermore, previous studies by our team have determined that neutrophils are a select population of blood cells that can bind to HPG under static conditions.[38] This likely reflects the difference in binding between high and low shear force for these cells.

Further analysis of the HPG coating was designed to establish suitable robustness and stability to survive packaging, sterilization, and long-term storage at ambient conditions. Packaging for nitinol stents involves high mechanical forces to first compress the stent, then slide it into the polymer sheath that keeps it compressed until deployment. The long-term stability of HPG-grafted nitinol stent sections was assessed over a 12-month period using the Chandler loop assay to test stored samples every 3 months (SI Figure 6). Preliminary results indicated that the HPG coating on stents retained its ability to prevent thrombosis for up to 12 months, when stored under ambient conditions. In a further study, full-length clinical grade stents (6 mm x 40 mm) were HPG-grafted, packaged, ethylene oxide-sterilized and stored under ambient conditions. Once again, stability of the coating was tested every 3 months for up to 12 months (SI Figure 7) and again at 44 months (SI Figure 9). The Chandler loop assay results in this repeat study confirm that the HPG coating is robust and able to retain its anti-thrombogenic properties throughout the packaging and sterilization process, which remained stable

for up to 44 months. Similar results were observed for much larger diameter HPG-grafted venous stents (14 mm x 60 mm) which were also packaged and sterilized (SI Figure 9).

Following on this encouraging demonstration of the HPG coating providing significant benefits to blood-contacting devices by reducing their thrombogenic potential, further investigations were necessary to determine if the HPG coating elicited any downstream effects, through activation of other pathways, above the level commonly seen for current implants.

Complement and neutrophils are not activated by HPG

The activation of complement and neutrophils on HPG-grafted stents was investigated using the Chandler loop model followed by testing of the blood from the loops, using an accredited testing laboratory to perform the analysis. For these experiments, blood was collected in lithium heparin Vacuette tubes (Greiner Bio-One International GmbH) to slow down clotting during testing. HPG-grafted stents were compared to uncoated nitinol stents. Two additional control samples were analyzed; blood that was added to a loop without any device present and blood that had not been exposed to the Chandler loop for 1 hour. The experiment was repeated with blood from five healthy donors. Results, summarized in Figure 4a, indicated no detectable loss of complement components for any of the tested samples. Complement component levels remained consistent across the samples but varied slightly between donors, with respect to pooled human reference serum. This analytical technique is highly sensitive to the loss of complement components that would indicate activation of the complement pathway. It was evident from these results that neither the uncoated control stents nor the HPG-grafted stents had activated the complement pathway, corroborating previous findings.[32] Furthermore, there was no significant difference between the samples with respect to reactive oxygen species (ROS) detection, which is an indicator of neutrophil activation (Figure 4b). All tested samples remained two orders of magnitude lower than the artificially activated sample that represented a serious clinical event. Therefore, it was concluded that neutrophils were not activated through transient contact with either the control or HPG-grafted stents under flow.

HPG-grafted materials do not elicit inflammatory responses *in vivo*

To explore potential adverse immune reactions triggered by the HPG coating once implanted into tissue, a pre-clinical rodent toxicity study was undertaken. HPG-grafted and bare nitinol disks implanted subcutaneously under the back skin of mice, for 1 or 5 weeks, were used to investigate potential acute and chronic inflammation, respectively. Histology on the explanted back skin that sat directly above the implanted disks indicated there was no significant alterations to overall thickness between the control disk, HPG-grafted disks and non-treated normal back skin after 1 or 5 weeks (Figure 5b). When each of the four layers, epidermis, stroma, muscle and fat were measured separately (Figure 5d-e), both the control disks and the HPG-grafted disks at 1 week showed a statistically significant increase in fat layer thickness, with respect to untreated back skin. However, there was no difference between fat layers of the control disks and the HPG-grafted disks. Furthermore, at 5 weeks the skin from the HPG-grafted disks had a significantly thinner fat layer than the normal untreated skin, while the uncoated control disk had returned to the same thickness as the normal untreated skin. While it was not expected that the bare nitinol disks would illicit an inflammatory response, this analysis confirms that the addition of an HPG coating does not induce an acute or chronic inflammatory reaction.

HPG-grafted stents reduce restenosis in (Apo)E$^{-/-}$ mice

Finally, we tested the effect of the HPG-coating on ISR using an *in vivo* model. We used the carotid inter-position grafting model in apolipoprotein (Apo)E$^{-/-}$ mice in which a stent is deployed into a donor descending thoracic aorta before grafting into the carotid artery of a recipient mouse, Figure 6a.[48] This study compared HPG-coated SS stents with bare SS stents over a period of 28 days. Analysis of the explanted stents, following fixation and sectioning, indicated that all control stents had become completely occluded (restenosed), largely by proliferating vascular smooth muscle cells, with resulting neointimal formation (Figure 6b). In stark contrast, HPG-coated stents had a large, fully patent lumen with minimal neointimal hyperplasia (Figure 6c). Neointima thickness measurements were taken to the center of the occluded control stents (500 μm) and found to be completely occluded along the entire length. The average area of restenosis for the control stents was 0.90 mm^2. The HPG-coated stents averaged a neointima thickness of 150 μm (measured from behind the stent strut to the edge of the new lumen), giving an average restenosis area of 0.34 mm^2 and remained patent along the entire length, resulting in a 62% reduction in restenosis over the bare control stents. Area of restenosis in HPG samples was measured by tracing the highly conserved tunica media (Figure 6f-g) and subtracting the area of the new lumen (SI Figure10). Area of restenosis for controls was measured from behind the stent struts but original vessel wall had to be estimated due to severe degradation of the tunica media in all samples Figure 6d-e).

DISCUSSION

With the advancements being made in stent design, the ongoing challenge is to create a stent coating that is ultrathin, safe, robust enough to withstand manufacturing processing and if possible devoid of drugs. A great deal of focus has been on novel device surface features such as chemistry, wettability and topography, aimed at having the least impact of the surrounding tissue.[23, 49] While there have been successful coatings developed, very few in

recent times have progressed into the clinic. Reasons include the integrity of nano-sized coatings, issues of scalability, biocompatibility and long-term stability that meets regulatory requirements.[50] Having succeeded in developing a simple method of creating a robust and stable HPG coating on metal stents we explored its potential as a safe antithrombogenic and antiproliferative coating.

Platelet adhesion and activation on implanted stents play a key role in ST and ISR. We were able to show that our HPG coating, when applied to various substrates, significantly reduced platelet binding by >99%. This was confirmed using platelets isolated from fresh human blood on both simple, flat surfaces as well as more complex structures, in a static model. Using the Chandler loop model to simulate blood flow, we showed that when applied to sections of a commercial nitinol stent, the HPG coating dramatically reduced the formation of clots on the stents compared to the uncoated sections. This was consistent across multiple experiments using different donor blood. When the surfaces were examined under high power magnification the lack of any attached and activated platelets or a fibrin network on the HPG-coated stent struts supported the lack of platelet binding observed in the initial static experiments.

Downstream effects of implanted materials that do not manifest at the site of the device are more difficult to correlate with a foreign-body-response but still pose a great risk to patients.[51] Two such effects are the activation of complement and neutrophils. The complement pathway can lead to thrombosis at the site of the device but can also trigger downstream effects through the generation of activated soluble factors that cause inflammatory responses in multiple organs with the kidneys being particularly susceptible to injury.[52] Similarly, neutrophil activation leads to the release of large quantities of reactive oxygen species (ROS) that can have devastating effects, such as vascular inflammation, atherosclerosis and even neuro-degeneration.[53-55] When fresh human blood exposed to the HPG-coated stents was further analyzed for evidence of activation of complement or neutrophils, the results showed our HPG coating could meet those hemocompatibility requirements.

Another key element to the foreign-body-response is inflammation, both acute and chronic, driven by the response of inflammatory cells, such as monocytes and neutrophils, to implanted device.[56] Migration of immune cells and fibroblasts to a wound site is a normal and necessary part of healing. However, implanted materials often disrupt this cycle of tissue repair leading to an imbalance of cell signaling factors and the continued influx of immune cells. Long-term effects may entail fibrous encapsulation of the device if matrix remodeling fibroblasts receive cues due to the presence of the implant. This is particularly problematic with synthetic polymers, even those commonly used in modern day surgical procedures, such as polypropylene mesh for hernia repair,[57] and silicone for breast implants.[58] To this end, it is critical to establish if the addition of the synthetic HPG coating triggers acute or chronic inflammation when implanted into tissue. This broader biocompatibility of the HPG coating was assessed using subcutaneously implanted nitinol disks that were coated and left for up to 5 weeks. The lack of any gross or microscopic evidence of an inflammatory response to either the bare nitinol or HPG-coated nitinol further illustrated the safety of this coating to the surrounding tissue. The same HPG polymer has been shown to be very safe in acute and chronic systemic toxicity studies in small rodents, which has been summarized in several recent reviews.[59, 60] Our results confirms that HPG grafted onto surfaces displays similar positive attributes of bio- and hemocompatibility when exposed to human blood, *ex vivo*.

Apart from ST, ISR can also reduce long-term stent patency. Restenosis is primarily caused by an inflammatory response as a result of stent deployment that stimulates the over-proliferation of medial (vessel wall) smooth muscle cells.[9-11, 16, 17] DES have significantly helped to overcome this clinical problem and are effective at reducing ISR, however limitations of DES have been documented over the years.[18, 50, 61] For example, in peripheral arterial disease, the benefits of drug coated devices have not been as dramatic as in coronary arterial disease, with the incidence of ISR in DES beyond 12 months returning to levels similar to bare metal stents.[61] Recent reports also suggest an increased risk of late all-cause mortality and amputations in patients treated with paclitaxel-eluting devices.[20, 22] With platelets playing a crucial role in ISR,[9, 15] our results with reduced platelet binding on HPG surfaces strongly suggested that our coating could also help prevent the onset of restenosis. In the established mouse model of ISR, we showed a substantial reduction in neointimal restenosis within the stented vessels of the HPG stent. While better understanding the mechanism of action is an area of ongoing research, the result is strongly suggestive of the benefit of our HPG coating to substantially reduce or prevent the cascade of inflammatory responses triggered by the insertion of stents that can lead to ISR.

In addressing commercial viability of our HPG coating, we investigated the robustness and stability of the coating on commercial stents. The initial results strongly suggest that our HPG coating can be applied uniformly to the surface of commercial metal stents in a reliable and consistent manner. The coating can withstand the normal manufacturing processing of a commercial stent, from coating through to the final sterile, packaged product. Furthermore, the coating has demonstrated stability up to 44 months, which suggests that a finished product with our coating would have adequate shelf-life stability to meet industry requirements.

The use of bare metal and drug-eluting stents has revolutionized the treatment of cardiovascular and peripheral vascular disease. Even so there remain significant unmet needs in the use of stents for delivering safe and durable relief for patients with vascular occlusions. The industry continues to advance stent technology, seeking new approaches that can promote reendothelialization and avoid restenosis without the need for cytotoxic agents. Through rigorous testing we have demonstrated in laboratory tests that our novel HPG coating has the qualities and properties of a truly biocompatible coating with tremendous potential to improve the performance of endovascular devices.

References

1. Iqbal, J., J. Gunn, and P.W. Serruys, *Coronary stents: historical development, current status and future directions.* British Medical Bulletin, 2013. **106**(1): p. 193-211.
2. Sakamoto, A., et al., *Understanding the Impact of Stent and Scaffold Material and Strut Design on Coronary Artery Thrombosis from the Basic and Clinical Points of View.* Bioengineering, 2018. **5**(3): p. 71.
3. Mariani, E., et al., *Biomaterials: Foreign Bodies or Tuners for the Immune Response?* International journal of molecular sciences, 2019. **20**(3): p. 636.
4. Werner, C., M. Maitz, and C. Sperling, *Current strategies towards hemocompatible coatings.* Journal of Materials Chemistry, 2007. **17**: p. 3376-84.
5. Li, Y.-H., et al., *2018 Expert Consensus on the Management of Adverse Effects of Antiplatelet Therapy for Acute Coronary Syndrome in Taiwan.* Acta Cardiologica Sinica, 2018. **34**(3): p. 201-210.
6. Degrauwe, S., et al., *Dual antiplatelet therapy for secondary prevention of coronary artery disease.* Open Heart, 2017. **4**(2): p. e000651.
7. Banerjee, S., et al., *Use of Antiplatelet Therapy/DAPT for Post-PCI Patients Undergoing Noncardiac Surgery.* Journal of the American College of Cardiology, 2017. **69**(14): p. 1861.
8. Spertus, J.A., et al., *Prevalence, Predictors, and Outcomes of Premature Discontinuation of Thienopyridine Therapy After Drug-Eluting Stent Placement.* Circulation, 2006. **113**(24): p. 2803-2809.
9. Mitra, A.K. and D.K. Agrawal, *In stent restenosis: bane of the stent era.* Journal of clinical pathology, 2006. **59**(3): p. 232-239.
10. Welt, F.G.P. and C. Rogers, *Inflammation and Restenosis in the Stent Era.* Arteriosclerosis, Thrombosis, and Vascular Biology, 2002. **22**(11): p. 1769-1776.
11. Gershlick, A.H. and J. Baron, *Dealing with in-stent restenosis.* Heart, 1998. **79**(4): p. 319-323.
12. Tadwalkar, R.V. and M.S. Lee, *The Current State of Endovascular Intervention for Peripheral Arterial Disease.* Vascular Disease Management, 2015. **12**(10): p. E190-E203.
13. Sanders, K.M., et al., *Endovascular treatment of high-risk peripheral vascular occlusive lesions: a review of current evidence and emerging applications of intravascular lithotripsy, atherectomy, and paclitaxel-coated devices.* Seminars in Vascular Surgery, 2021. **34**(4): p. 172-187.
14. Sarwar, U., et al., *Brief Review of Options to Treat In-stent Restenosis of Femoro-popliteal Artery.* International Journal of Cardiology and Cardiovascular Disorder, 2021. **2**(3): p. 1-4.
15. Haybar, H., M.S.S. Pezeshki, and N. Saki, *Platelets in In-stent Restenosis: From Fundamental Role to Possible Prognostic Application.* Current Cardiology Reviews, 2020. **16**(4): p. 285-291.
16. Tan, R.P., et al., *Macrophage Polarization as a Novel Therapeutic Target for Endovascular Intervention in Peripheral Artery Disease.* JACC: Basic to Translational Science, 2021. **6**(8): p. 693-704.
17. Maleknia, M., et al., *Inflammatory Growth Factors and In-Stent Restenosis: Effect of Cytokines and Growth Factors.* SN Comprehensive Clinical Medicine, 2020. **2**: p. 1-11.
18. van der Hoeven, B.L., et al., *Drug-eluting stents: results, promises and problems.* International Journal of Cardiology, 2005. **99**(1): p. 9-17.
19. Bavry, A.A., et al., *Late Thrombosis of Drug-Eluting Stents: A Meta-Analysis of Randomized Clinical Trials.* The American Journal of Medicine, 2006. **119**(12): p. 1056-1061.
20. Katsanos, K., et al., *Risk of Death Following Application of Paclitaxel-Coated Balloons and Stents in the Femoropopliteal Artery of the Leg: A Systematic Review and Meta-Analysis of Randomized Controlled Trials.* Journal of the American Heart Association, 2018. **7**(24): p. e011245.
21. Behrendt, C.A., et al., *Long Term Survival after Femoropopliteal Artery Revascularisation with Paclitaxel Coated Devices: A Propensity Score Matched Cohort Analysis.* Eur J Vasc Endovasc Surg, 2020. **59**(4): p. 587-596.
22. Zeller, T., et al., *Drug-Eluting Balloon Versus Standard Balloon Angioplasty for Infrapopliteal Arterial Revascularization in Critical Limb Ischemia: 12-Month Results From the IN.PACT DEEP Randomized Trial.* Journal of the American College of Cardiology, 2014. **64**(15): p. 1568-1576.
23. Beshchasna, N., et al., *Recent Advances in Manufacturing Innovative Stents.* Pharmaceutics, 2020. **12**(4): p. 349.
24. Moore, E., et al., *Surface-Initiated Hyperbranched Polyglycerol as an Ultralow-Fouling Coating on Glass, Silicon, and Porous Silicon Substrates.* ACS Applied Materials & Interfaces, 2014. **6**(17): p. 15243-15252.
25. Moore, E., et al., *Patterning and Biofunctionalization of Antifouling Hyperbranched Polyglycerol Coatings.* Biomacromolecules, 2014. **15**(7): p. 2735-2743.
26. Höger, K., et al., *Polyglycerol coatings of glass vials for protein resistance.* European Journal of Pharmaceutics and Biopharmaceutics, 2013(0).
27. Siegers, C., M. Biesalski, and R. Haag, *Self-assembled monolayers of dendritic polyglycerol derivatives on gold that resist the adsorption of proteins.* Chemistry – A European Journal, 2004. **10**(11): p. 2831-8.
28. Weinhart, M., et al., *Linear and Hyperbranched Polyglycerol Derivatives as Excellent Bioinert Glass Coating Materials.* Advanced Engineering Materials, 2011: p. B501-B510.
29. Chen, P.-R., et al., *Development of Antifouling Hyperbranched Polyglycerol Layers on Hydroxyl Poly-p-xylylene Coatings.* Langmuir, 2017. **33**(51): p. 14657-14662.
30. Kainthan, R.K. and D.E. Brooks, *In vivo biological evaluation of high molecular weight hyperbranched polyglycerols.* Biomaterials, 2007. **28**(32): p. 4779-4787.
31. Kainthan, R.K., et al., *In vitro biological evaluation of high molecular weight hyperbranched polyglycerols.* Biomaterials, 2007. **28**(31): p. 4581-4590.
32. Kainthan, R.K., et al., *Biocompatibility Testing of Branched and Linear Polyglycidol.* Biomacromolecules, 2006. **7**(3): p. 703-709.
33. Chapanian, R., et al., *In vivo circulation, clearance, and biodistribution of polyglycerol grafted functional red blood cells.* Biomaterials, 2012. **33**(10): p. 3047-3057.
34. Kulka, M.W., et al., *Surface-Initiated Grafting of Dendritic Polyglycerol from Mussel-Inspired Adhesion-Layers for the Creation of Cell-Repelling Coatings.* Advanced Materials Interfaces, 2020. **7**(24): p. 2000931.
35. Weber, T., Y. Gies, and A. Terfort, *Bacteria-Repulsive Polyglycerol Surfaces by Grafting Polymerization onto Aminopropylated Surfaces.* Langmuir, 2012. **28**(45): p. 15916-15921.
36. Khan, M. and W.T.S. Huck, *Hyperbranched Polyglycidol on Si/SiO2 Surfaces via Surface-Initiated Polymerization.* Macromolecules, 2003. **36**(14): p. 5088-5093.
37. Wei, Q., et al., *Multivalent Anchoring and Cross-Linking of Mussel-Inspired Antifouling Surface Coatings.* Biomacromolecules, 2014. **15**(8): p. 3061-3071.

38. Burzava, A.L.S., et al., *Surface-Grafted Hyperbranched Polyglycerol Coating: Varying Extents of Fouling Resistance across a Range of Proteins and Cells.* ACS Applied Bio Materials, 2020. **3**(6): p. 3718-3730.

39. Aslan, J.E., et al., *Platelet Shape Change and Spreading*, in *Platelets and Megakaryocytes: Volume 3, Additional Protocols and Perspectives*, J.M. Gibbins and M.P. Mahaut-Smith, Editors. 2012, Springer New York: New York, NY. p. 91-100.

40. Lee, D., et al., *Differential Dynamics of Platelet Contact and Spreading.* Biophysical Journal, 2012. **102**(3): p. 472-482.

41. Leslie, D.C., et al., *A bioinspired omniphobic surface coating on medical devices prevents thrombosis and biofouling.* Nature Biotechnology, 2014. **32**: p. 1134.

42. Qiu, Y., et al., *Platelet mechanosensing of substrate stiffness during clot formation mediates adhesion, spreading, and activation.* Proceedings of the National Academy of Sciences of the United States of America, 2014. **111**(40): p. 14430-14435.

43. Sheth, S., et al., *Subacute Thrombosis and Vascular Injury Resulting From Slotted-Tube Nitinol and Stainless Steel Stents in a Rabbit Carotid Artery Model.* Circulation, 1996. **94**(7): p. 1733-1740.

44. Chandler, A.B., *In vitro thrombotic coagulation of the blood; a method for producing a thrombus.* Lab Invest, 1958. **7**(2): p. 110-4.

45. Zhang, W., et al., *Chandler-Loop surveyed blood compatibility and dynamic blood triggered degradation behavior of Zn-4Cu alloy and Zn.* Materials Science and Engineering: C, 2021. **119**: p. 111594.

46. Hopkins, C., et al., *Webbing and Delamination of Drug Eluting Stent Coatings.* Ann Biomed Eng, 2016. **44**(2): p. 419-31.

47. Ng, J., et al., *Local Hemodynamic Forces After Stenting.* Arteriosclerosis, Thrombosis, and Vascular Biology, 2017. **37**(12): p. 2231-2242.

48. Ali, Z.A., et al., *Increased In-Stent Stenosis in ApoE Knockout Mice.* Arteriosclerosis, Thrombosis, and Vascular Biology, 2007. **27**(4): p. 833-840.

49. Zhao, J. and Y. Feng, *Surface Engineering of Cardiovascular Devices for Improved Hemocompatibility and Rapid Endothelialization.* Adv Healthc Mater, 2020. **9**(18): p. e2000920.

50. Cherian, A.M., et al., *Surface engineering at the nanoscale: A way forward to improve coronary stent efficacy.* APL Bioengineering, 2021. **5**(2): p. 021508.

51. Schoen, F.J. and A.S. Hoffman, *Chapter III.1.4 - Device Failure Mode Analysis*, in *Biomaterials Science (Third Edition)*, B.D. Ratner, et al., Editors. 2013, Academic Press. p. 1361-1368.

52. Noris, M. and G. Remuzzi, *Overview of complement activation and regulation.* Seminars in nephrology, 2013. **33**(6): p. 479-492.

53. Nguyen, G.T., E.R. Green, and J. Mecsas, *Neutrophils to the ROScue: Mechanisms of NADPH Oxidase Activation and Bacterial Resistance.* Frontiers in Cellular and Infection Microbiology, 2017. **7**(373).

54. Uttara, B., et al., *Oxidative Stress and Neurodegenerative Diseases: A Review of Upstream and Downstream Antioxidant Therapeutic Options.* Current Neuropharmacology, 2009. **7**(1): p. 65-74.

55. Kattoor, A.J., et al., *Oxidative Stress in Atherosclerosis.* Curr Atheroscler Rep, 2017. **19**(11): p. 42.

56. Hannan, R.T., S.M. Peirce, and T.H. Barker, *Fibroblasts: Diverse Cells Critical to Biomaterials Integration.* ACS biomaterials science & engineering, 2018. **4**(4): p. 1223-1232.

57. Heymann, F., et al., *Polypropylene mesh implantation for hernia repair causes myeloid cell-driven persistent inflammation.* JCI insight, 2019. **4**(2): p. e123862.

58. Shin, B.H., et al., *Silicone breast implant modification review: overcoming capsular contracture.* Biomaterials Research, 2018. **22**(1): p. 37.

59. Abbina, S., et al., *Hyperbranched polyglycerols: recent advances in synthesis, biocompatibility and biomedical applications.* Journal of Materials Chemistry B, 2017. **5**(47): p. 9249-9277.

60. Jafari, M., et al., *Hyperbranched polyglycerol nanostructures for anti-biofouling, multifunctional drug delivery, bioimaging and theranostic applications.* International Journal of Pharmaceutics, 2020. **576**: p. 118959.

61. Kokkinidis, D.G. and E.J. Armstrong, *Current developments in endovascular therapy of peripheral vascular disease.* J Thorac Dis, 2020. **12**(4): p. 1681-1694.

62. Griesser, H.J., *Small-Scale Reactor for Plasma Processing of Moving Substrate Web.* Vacuum, 1989. **39**(5): p. 485-488.

63. Cazenave, J.-P., et al., *Preparation of Washed Platelet Suspensions From Human and Rodent Blood*, in *Platelets and Megakaryocytes: Volume 1: Functional Assays*, J.M. Gibbins and M.P. Mahaut-Smith, Editors. 2004, Humana Press: Totowa, NJ. p. 13-28.

64. Ali, Z.A., et al., *Gene Transfer of a Broad Spectrum CC-Chemokine Inhibitor Reduces Vein Graft Atherosclerosis in Apolipoprotein E-Knockout Mice.* Circulation, 2005. **112**(9_supplement): p. I-235-I-241.

Acknowledgments

Author Contributions

E.M., T.S., G.B. and C.S.B. conceived the study. E.M., A.B., M.C. designed, performed and analyzed the experiments, interpreted data and generated figures. M.C. and V.N. performed *in vivo* experiments. M.C. collected human blood. M.T., P.J.P., J.W.F. and T.S. interpreted data. C.S.B., C.B., H.J.G. and N.H.V. designed experiments and interpreted data. M.T. generated figures. E.M. wrote the manuscript with input from all authors.

Ethics declarations

Competing interests: T.S. is the CEO and shareholder of TekCyte Limited, which is commercializing HPG coatings. E.M. is employed 0.2 FTE by TekCyte Limited. E.M. C.S.B, G.B. and N.H.V. are inventors on patents involving the HPG coating process (WO2017156592 and WO2017156593). All other authors have nothing to declare.
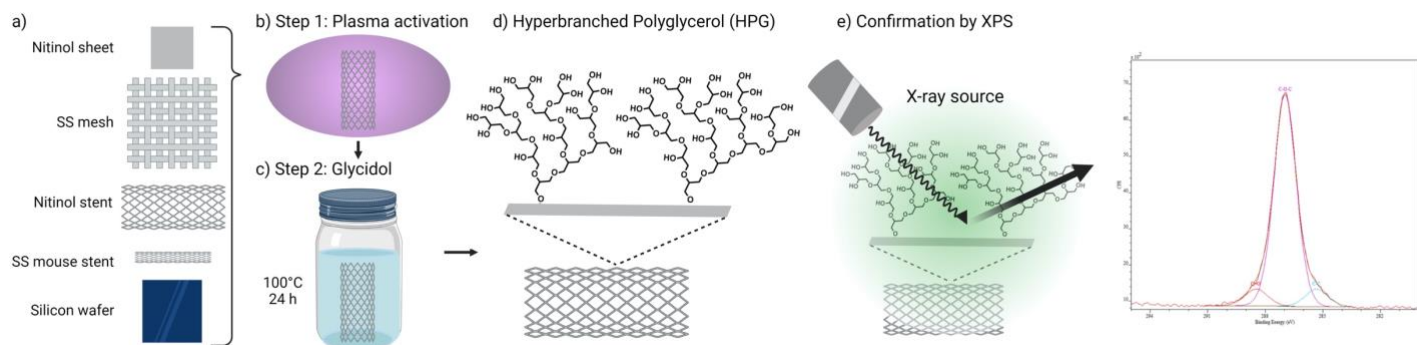
Figure 1. **Graphical overview of HPG the coating process.** a) Different materials (nitinol sheet and stent, stainless-steel (SS) mesh and mouse stent, and silicon wafer spin-coated with polystyrene) were successfully coated with HPG. b) The first step of process is activating the material with plasma followed by c) incubation in glycidol at 100ᵒC for 24 hours leading to the d) growth of a nano-thin layer of hyperbranched polyglycerol. e) Successful HPG coating was confirmed by X-ray photoelectron spectroscopy (XPS). (Created with BioRender.com)
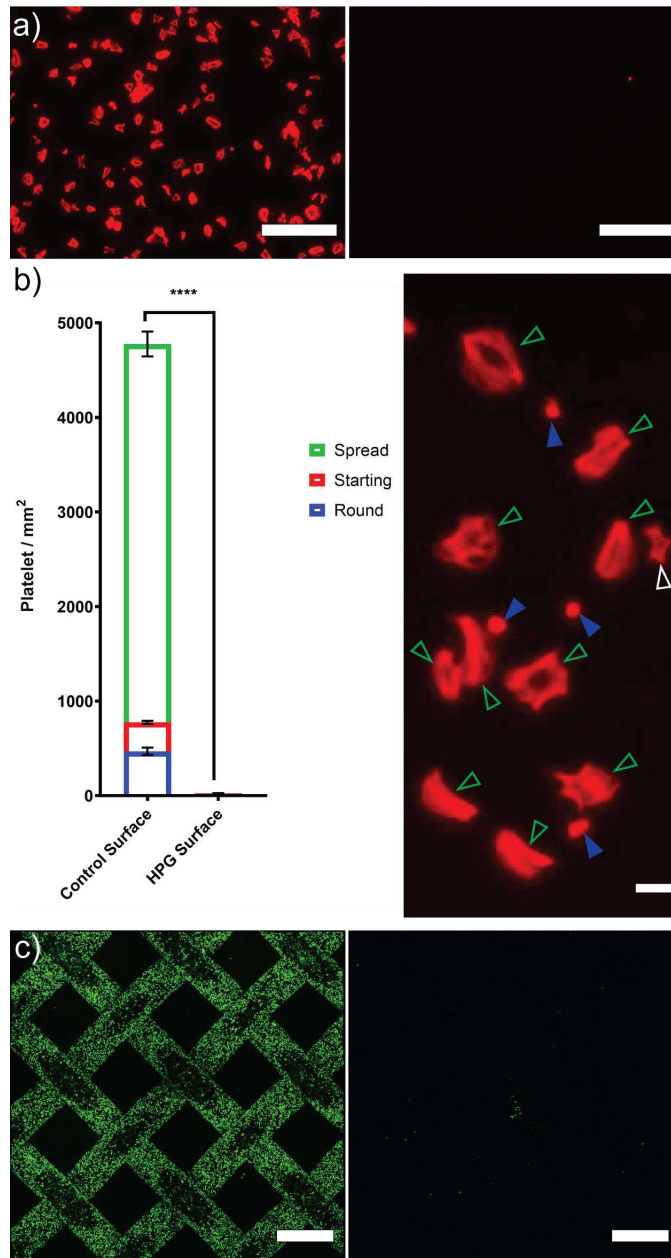
Figure 2. **Platelet binding.** a) Platelets isolated from human blood bind to plasma-treated polystyrene (PS) but not HPG-coated surfaces. Scale bar indicates 40 μm. b) Quantification of platelets (spread in green, starting in red, and round in blue) bound to PS and HPG surfaces. ****= p ≤ 0.0001. Examples of spread (green hollow arrowheads), starting to spread (white hollow arrowheads) and round (blue solid arrowheads) morphologies (Scale bar indicates 5 μm). c) Human platelets bind to a stainless-steel (SS) mesh (left) but not to HPG-coated SS mesh. Scale bar indicates 200 μm. A two-tailed unpaired Student's t test was performed to determine statistical significance between groups with p values <0.05 considered significant.
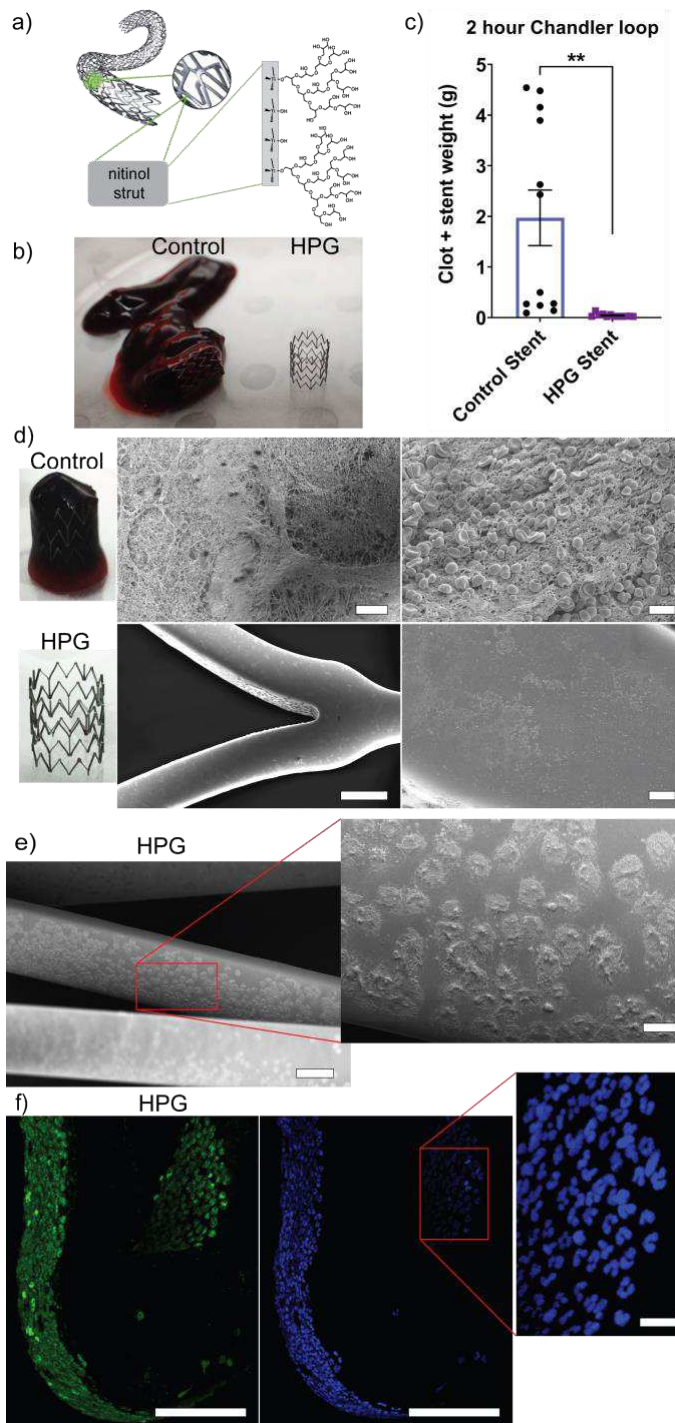
Figure 3. **HPG–coated stents prevent platelet binding.** a) Schematic of a stent made from nitinol struts coated with Hyperbranched Polyglycerol. b) HPG coating prevents blood from clotting in a Chandler loop. c) Comparison of combined weight of clot and stent of a control stent vs an HPG-coated stent after two hours in a Chandler loop. Error bars = mean with SEM, n=12, **= p ≤ 0.01. d) Magnified images of control and HPG stent, and electron microscope images of platelets and fibrin networks bound to them. Scale bars indicate 100 μm (centre images) and 10 μm (right images). e) Cells predominantly bind to strut areas that are perpendicular to the blood flow. Scale bars indicate 100 μm (left) and 20 μm (right). f) Fluorescence microscopy images of lobulated mononuclear cells consistent with neutrophils bound to HPG-coated stent struts. Cells were stained with CFDA SE Cell Tracer in green and DAPI in blue. Scale bars indicate 100 μm (left and middles) and 15 μm (right).
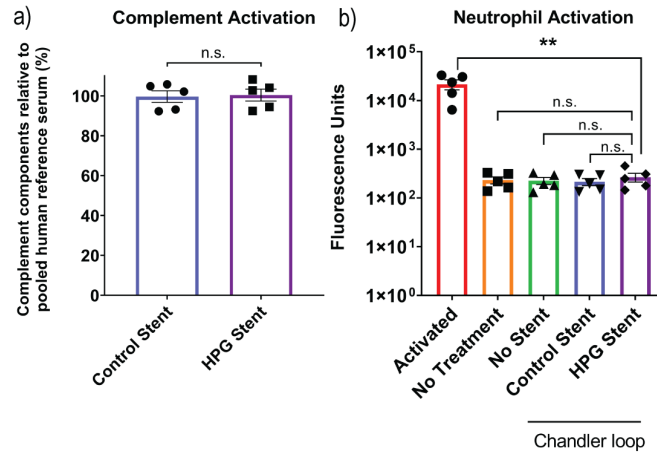
Figure 4. **HPG-coated stents do not trigger an inflammatory response.** a) There is no significant difference between the control stent and HPG stent compared to the pooled human reference serum. n.s. not significant. b) The detected reactive oxygen species are significantly lower in the controls and HPG stent than the activated control. Mean with SEM, n=5, **= p ≤ 0.01. A two-tailed unpaired Student's t test was performed to determine statistical significance between groups with p values <0.05 considered significant.
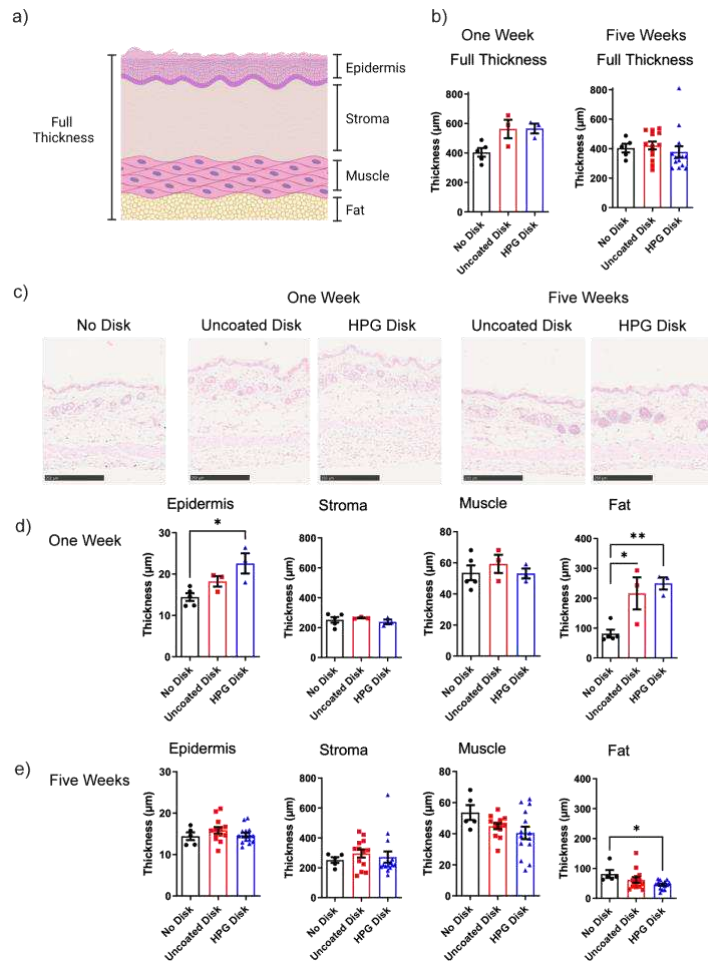
Figure 5. **HPG coating does not elicit an inflammatory response *in vivo*.** a) Schematic of cross section through murine back skin created with BioRender.com. b) Analyzed full skin thickness following one and five-week time points with uncoated (red) and HPG-coated nitinol disks (blue) compared to back skin of mice which received no disk (black). Mean with SEM, n=3-15, *= p ≤ 0.05, **= p ≤ 0.01. c) Representative images of sections stained with H&E after one and five weeks. Scale bars indicate 250 μm. d) and e) Analyzed thickness for each individual skin layer for one and five weeks, respectively. A two-tailed unpaired Student's t test was performed to determine statistical significance between groups with p values <0.05 considered significant.
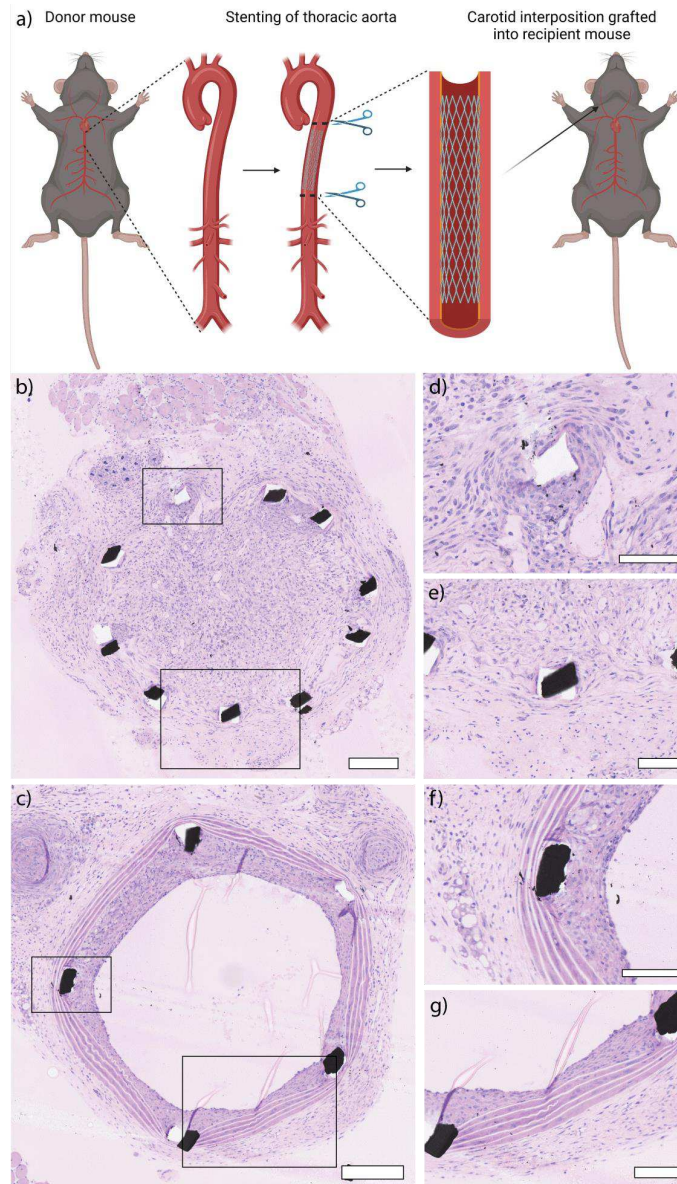
Figure 6 **HPG-grafted stents reduce restenosis in ApoE$^{-/-}$ mice.** a) Graphical overview of mouse surgery created with BioRender.com. A SS stent was inserted retrograde up the thoracic aorta of an ApoE$^{-/-}$ donor mouse. The aorta was harvested and ligated into the carotid artery of a recipient ApoE$^{-/-}$ mouse. After 28 days of chow diet, the blood vessels containing the stents were removed, fixed and resin embedded. b) In all controls, stent lumen is completely occluded by neointimal, largely smooth muscle cells, hyperplasia and struts are surrounded by a significant epithelioid macrophage and multinucleated giant cell (foreign body granulomatous) reaction (n=3). By contrast c) the HPG-coated stents have a large patent lumen with minimal neointimal formation. The granulomatous reaction to the struts is greatly reduced compared to controls (n=2). Black structures within the vessels are stent struts. Scale bars indicate 200 μm in images on the left (b-c), and 100 μm in the magnified images (d-g). Sections stained with H&E.

Methods

Modification of substrates with HPG. For **HPG-grafted** polystyrene (PS) samples, silicon wafers were cut into 1 cm^2 pieces, and cleaned using the Radio Corporation of America (RCA) critical process guidelines. In short, samples were treated for 30 minutes at 70 °C with a 1:1:5 ratio of ammonium hydroxide, hydrogen hydroxide and MilliQ water respectively. They were then washed twice with MilliQ water before being immersed and sonicated for 5 minutes in ethanol followed by acetone. Clean silicon wafers were stored in acetone before use. Before doing the spin coating, a solution 1.75% of polystyrene (PS) by weight was made by dissolving polystyrene beads in toluene at 50°C for 2 hours. Silicon wafers were dried with a stream of N$_2$. Each sample was subsequently coated with 100 μL of the polystyrene solution using a spin coater at the rate of 3000 rpm for 40 seconds. PS-coated silicon pieces were then activated with air plasma in a custom-built reactor similar to the one described previously [62]. Plasma activation was carried out under application of continuous RF power of 100 W for 5 minutes, with air pressure during treatment at 3×10^{-2} mbar. Samples were immediately immersed in distilled glycidol after plasma activation and left to polymerize in an oven at 100 °C for 24 hours. Polymerization was terminated by removing the unreacted monomer solution and quenching the reaction by a succession of three 5 minutes washes with methanol under light agitation. Before further analysis, samples were thoroughly washed with PBS (every 15 minutes for 3-4 hours). An additional washing with MilliQ water was performed for another 2 hours and samples were dried with a stream of N$_2$ if they were to be studied for surface analysis. **HPG-grafted stainless-steel (SS) mesh, nitinol stents, nitinol sheet and SS mouse stents** were prepared as follows. Substrates were gently agitated in 100% isopropanol (Thermo Fisher Scientific) for three 5 min washes. Substrates were then dried under a stream of N$_2$ and activated with argon plasma in a Diener Femto plasma cleaner. Plasma activation was carried out under application of continuous LF power of 100 W for 20 minutes, with argon pressure during treatment at 6×10^{-2} mbar. Following plasma treatment, the vacuum chamber was backfilled with argon gas and the substrates immediately immersed in distilled glycidol and left to polymerize in an oven at 100 °C for 24 hours. Polymerization was terminated by removing the unreacted monomer solution and quenching the reaction by a succession of three 5 minutes washes with methanol under light agitation. HPG-grafted substrates were dried under a stream of N$_2$ and stored under ambient conditions until use.

Elemental analysis. X-ray photoelectron spectroscopy (XPS) was performed with a Kratos AXIS Ultra DLD spectrometer, using monochromatic AlKα radiation (hv = 1486.7 eV). The system is equipped with a magnetically confined charge compensation system (low energy electrons are confined and transported to the sample surface by magnetic field). Spectra were recorded using an acceleration voltage of 15 keV at a power of 225 W. Survey spectra were collected with a pass energy of 160 eV and an analysis area of 300×700 μm^2. High-resolution spectra were obtained using a 20 eV pass energy and an analysis area of 300×700 μm^2. Data analysis was performed with CasaXPS software (Casa Software Ltd.). All binding energies were referenced to the low energy C 1s peak at 285.0 eV. Core level envelopes were curve-fitted with the minimum number of mixed Gaussian–Lorentzian component profiles. The Gaussian–Lorentzian mixing ratio (typically 30% Lorentzian and 70% Gaussian functions) the full width at half-maximum, and the positions and intensities of peaks were left unconstrained to result in a best fit.

Ethics

The collection of peripheral blood from healthy individuals was approved by the Human Research Ethics Committees (HREC) of the Royal Adelaide Hospital (#130308 and #201187), the University of South Australia (#200585) and the University of New South Wales (HC14108). Animal studies were approved by animal ethics committees of SA Pathology & University of South Australia (#18-16) as well as the South Australian Health and Medical Research Institute (SAHMRI).

Isolated platelet assays. Platelet assays on **flat PS** were performed with the help of Dr Jelena Rnjak-Kovacina and Kieran Lau at the University of New South Wales (UNSW) and were approved by the ethics board (HC14108) of UNSW (Australia).
Blood was collected from a healthy donor, put in vacutainers containing 3.2% trisodium citrate as an anti-coagulant (Becton Dickson, Macquarie Park, NSW, AU) and used straight away. The upper platelet-rich plasma was aspirated after a 160 g centrifugation for 15 min, and centrifuged again at 340 g for 15 min. The platelet pellet was then resuspended in Tyrode's buffer (Sigma-Aldrich, St Louis, MO, USA) with 0.1 U/ml apyrase. Particular care was given to limit any shear stress and agitation in order to prevent platelet activation during the isolation process. Platelets were seeded at 5×10^6 platelets/well onto each sample material and incubated for 1h at 37 °C. Platelets were fixed with 4% paraformaldehyde solution with 1% sucrose for 15 min, and then permeabilized with 300 mM sucrose, 50 mM NaCl, 3 mM MgCl$_2$, 2 mM HEPES, 0.5% Triton X-100, pH 7.2 for 5 min at 4°C and blocked in 1% BSA in PBST (PBS containing 0.05% Tween-20) for 1h at room temperature. Two PBS washes were performed between each of the above steps. Samples were stained with rhodamine phalloidin (Life Technologies, Carlsbad, CA, USA) at 1:200 dilution ratio for 1h at 37 °C. Finally, samples were rinsed twice with PBST, before being fixed onto a glass slide with a droplet of Fluoromount aqueous mounting medium covered by a glass coverslip deposited on each sample. Samples were stored in the dark before imaging.

Platelet assays on **SS mesh** was performed with the help of Dr Carmela Martini. Blood from healthy donors (aged 18–65 years, non-smokers and aspirin/NSAIDs free for at least 1 month) was collected into acid-citrate dextrose (ACD, pH 4.5) anticoagulant and platelets purified as described elsewhere [63]. Briefly, blood was collected from single donors, rested at RT for 15 min prior to 180 g centrifugation, the platelet-rich-plasma was then centrifuged at 1,100 g for 15 min and the platelet pellet was resuspended gently with Tyrode's platelet wash buffer (137 mM NaCl, 2.7 mM KCl, 1mM MgCl$_2$.6H$_2$O, 12 mM NaHCO$_3$, 0.4 mM NaH$_2$PO$_4$.H$_2$O, 3.7 mM HEPES, pH 7.4) containing 1.78U/mL Apyrase (BD Biosciences, San Jose, CA, USA). The platelet suspension was incubated at 37 °C for 5 min, centrifuged at $1,100 \times g$ for 15 min then resuspended in Tyrode's platelet resuspension buffer (Tyrode's wash buffer, 3 mM CaCl$_2$) containing 0.178U/mL Apyrase. Platelets were counted using a Sysmex XE-5000 differential analyzer (Sysmex Corporation, Kobe, Japan) and validated for purity and low-level activation via flow cytometric analysis. Platelets were stained with anti-CD42b and anti-CD62P or isotype-matched control antibody (all BD Biosciences, Ann Arbor, MI, USA) for 15 min with samples processed by a BD Accuri C6 flow cytometer with subsequent analyses performed on FCS Express 6 cytometry software (De Novo Software, Glendale, CA, USA).

Platelets were seeded at 3×10^6 platelets/well, in platelet suspension buffer, onto each sample material and incubated for 2.5h at 37 °C. Samples were then washed lightly once with PBS and fixed with paraformaldehyde (4% in PBS) for 15 minutes at room temperature. Three PBS washes were performed following fixing of the samples then adhered platelets were stained with CFDA SE cell tracer (Thermo Fisher Scientific) at 1:2000 dilution ratio for 20 minutes at 37 °C. Finally, samples were rinsed three times with PBS and three times with MilliQ water then stored in the dark before imaging.

Chandler loop assay. Non-packaged stent sections, both control and HPG-coated were rinsed in RO water three times for 5 minutes each and then sterile PBS three times for 5 minutes each in a biosafety cabinet. Washed samples were removed from the PBS and placed individually into lengths of Tygon ND-100-65 tubing. The tubes were sealed in a loop using an out cuff that held the two ends firmly together. Sticky tape was also applied to the ends of the cuff to ensure it did not come apart. Each tube was slid over a plastic container that acted as the drum of the rotator and taped in place. A 19G and 26G needle were placed into each tube to enable blood to be injected in (19G) while allowing air to escape (26G).

50 mL of healthy human blood was collected in the lab into a syringe preloaded with Heparin (0.5 U/mL blood) diluted into 1 mL PBS. The blood was injected into the loops within 2 minutes of collection, leaving a ~2 cm long air bubble at the top of each loop. Needles were removed from the loops and tape was applied over the puncture sites to prevent leakage. The loops were rotated at 175/s (~5 dyn/cm^2) for 2 h and up to 4.5 h, at 37°C. At the conclusion of the assay, loops were cut open and the contents of each was collected. Clots in stents was blotted on paper to remove liquid blood and placed in pre-weighed tubes. Stents with little or no clot were dipped in PBS 5 times to remove unbound blood before being blotted dry on paper towel and placed in pre-weighed tubes. The weight of each stent and associated clot was recorded. Stents were then cut away from protruding clots and all

devices were fixed in PFA over night at room temperature. Following fixation, stents were washed once with PBS, once with RO water and then placed in ethanol (80% V/V).

Scanning electron microscopy. Fixed stents were dehydrated (80% EtOH 24h, 90% EtOH 24 h, 100% EtOH 24h) and dried (50:50 solution of EtOH and Hexamethyldisilazane (Sigma-Aldrich) for 20 mins and finally 100% Hexamethyldisilazane for 20 min prior to air drying) prior to sputter coating with 10 nm platinum in a Cressington 208 HR sputter coater (Cressington, Watford, UK) using an Argon (BOC, North Ryde, Australia) plasma and platinum sputter target (ProSciTech, Thuringowa Central, Australia). Samples were examined under a scanning electron microscope (Crossbeam 540 with GEMINI II column, Carl Zeiss, Oberkochen, Baden-Wurttemberg, Germany) equipped with a field emission gun operated at 3 kV, a 100 pA probe current applied and secondary electron images recorded with an Inlens Secondary Electron detector.

Complement and neutrophil activation. Complement and neutrophil activation assays were performed by SA Pathology as a fee for service following accredited protocols outlined in internal documents PRC-IMI-020-REV2 and PRC-IMP-157, respectively. In short, complement activity was measured from donor serum and compared to a reference of pooled serum from 3 human donors using the CH50 assay. Neutrophil activation was measured from isolated cells using the dihydrorhodamine-123 oxidative burst assay with phorbol myristate acetate (PMA) added to one sample as a positive control. For each of 5 healthy donors, of various age and sex, 5 x 9 mL blood was collected in Vacuette® lithium heparin tubes. One tube of blood was retained as a native blood control that had not been subjected to the Chandler loop conditions. The remaining four tubes were combined, and 10 mL of heparinised blood loaded into 3 prepared loops as described above for the Chandler loop assay. One loop contained no stent sample and acted as a control for activation via handling, exposure to the tube material and flow conditions. The two remaining loops contained either a bare control stent or a HPG coated stent. All three loops were sealed and run as described previously for 1 hour. Following exposure for 1 hour, the blood was collected from the loops and taken, at room temperature, for testing. All testing was performed within 2.5 hours of collection from donors.

in vivo inflammatory response model
Female Balb/c mice aged 6-8 weeks were sourced from the Animal Resource Centre (Perth, Australia), and housed under conventional conditions. A 1cm incision was made in the skin along the midline of the back and blunt dissection was used to create a pocket under the skin on each flank for disk. Each mouse received an HPG-coated and bare uncoated nitinol disk 5mm in diameter under the skin of each flank with sides randomised. For the coated disks the coating side was placed facing the skin. After checking disk placement, the midline incision was closed with 4.0 PDL II sutures (Source). Disks remained embedded for either one or five weeks. At the endpoint, the skin above each disk was inspected for signs of inflammation and the disk was removed along with the skin in contact with the disk, approximately 10mm x 10mm. Skin sections were fixed in 10% buffered formalin (source) and paraffin embedded.

Formalin fixed paraffin embedded skin sections were cut to 8 μm, dewaxed and stained with hematoxylin and eosin to show skin morphology and signs of inflammation. Stained slides were scanned on a NanoZoomer 2.0-HT (Hamamatsu, Japan) and blinded before analysis with NDP.view software (Hamamatsu). Measurements were taken of the width of the Epidermis, dermis, muscle and adipose layers along with the full skin thickness at two separate points on the section for 2-4 separate sections of skin per mouse. Results were analysed and graphed in Prism (Graphpad, CA, USA) and compared to back skin from normal Balb/c mice that did not receive a disk or surgery.

Carotid interposition graft model of stenting. The surgical procedure was performed as previously described.[48, 64] In chow-fed, 10- to 14-week-old male ApoE$^{-/-}$ donor mice, a SS stent (2.5 x 0.6 mm; Brivant Ltd., Galway, Ireland) was crimped onto a 1.25 x 0.6-mm balloon angioplasty catheter (Medtronic, Milwaukee, Wisconsin). This was inserted retrograde up the thoracic aorta of the donor mouse through a small transverse arteriotomy made marginally superior to the diaphragmatic outlet and the balloon inflated to an atmospheric pressure of 12 Pa for 30 s. The aorta (~10 to 15 mm in length) was harvested by sealing the intercostal branch vessels with electrocautery. The harvested aortas did not exceed a total ischemic time of 15 min and were stored in PBS.

In the recipient mouse, the right common carotid artery was ligated and divided between 7-0 silk ties at its midpoint. Polyethylene cuffs (0.65-mm diameter) were placed over each end and anchored by clamps. The artery was everted over the cuffs and secured with 8-0 silk sutures. The donor aorta was then interposition-grafted by sleeving its ends over the carotid artery cuffs and secured using 8-0 silk sutures. Vessel patency was checked by removing the clamps and restoring blood flow to the vessel. Mice received aspirin (10 mg/kg/day) in drinking water for 1 week before surgery and post-surgery for 28 days to reduce the risk of in-stent thrombosis.

Resin embedding of stented vessels. Stented vessels were harvested 28 days after surgery and perfused in situ with 4% phosphate-buffered paraformaldehyde, then excised and embedded into JB-4 (glycol methacrylate) resin (ProSciTech, Thuringowa Central, Australia) according to the manufacturer's instructions for histomorphometry and immunohistochemistry analysis. Transverse sections (5 μm) of the stent were cut using a tungsten-carbide blade on an automatic microtome.

In-stent neointimal hyperplasia quantification. For histomorphometric analysis, resin-embedded samples were stained with hematoxylin and eosin then imaged on a Hamamatsu Photonics NanoZoomer whole slide imaging microscope. The total neointimal area was quantified in NDP.view 2 software on 5 stented sections/vessel by taking the area inside the internal elastic lamina, minus the lumen. An additional measurement was performed that looked at the stent strut to the edge of the lumen distance (4 to 6 measurements/section).

1.   Griesser, H.J., *Small-Scale Reactor for Plasma Processing of Moving Substrate Web.* Vacuum, 1989. **39**(5): p. 485-488.
2.   Cazenave, J.-P., et al., *Preparation of Washed Platelet Suspensions From Human and Rodent Blood*, in *Platelets and Megakaryocytes: Volume 1: Functional Assays*, J.M. Gibbins and M.P. Mahaut-Smith, Editors. 2004, Humana Press: Totowa, NJ. p. 13-28.
3.   Ali, Z.A., et al., *Gene Transfer of a Broad Spectrum CC-Chemokine Inhibitor Reduces Vein Graft Atherosclerosis in Apolipoprotein E-Knockout Mice.* Circulation, 2005. **112**(9_supplement): p. I-235-I-241.
4.   Ali, Z.A., et al., *Increased In-Stent Stenosis in ApoE Knockout Mice.* Arteriosclerosis, Thrombosis, and Vascular Biology, 2007. **27**(4): p. 833-840.

Supplementary Files

This is a list of supplementary files associated with this preprint. Click to download.

- MooreetalSupportingInformation.pdf